On the Relation of the LHeC and the LHC

LHeC Study Group [1]

Abstract

The present note relies on the recently published conceptual design report of the LHeC and extends the first contribution to the European strategy debate in emphasizing the role of the LHeC to complement and complete the high luminosity LHC programme. The brief discussion therefore focusses on the importance of high precision PDF and α_s determinations for the physics beyond the Standard Model (GUTs, SUSY, Higgs). Emphasis is also given to the importance of high parton density phenomena in nuclei and their relevance to the heavy ion physics programme at the LHC.

Submitted to the European Strategy for Particle Physics,
October 2012.

---

[1]For the current author list see the end of this note. Contacts: oliver.bruning@cern.ch and max.klein@cern.ch

1 Introduction

Deep inelastic lepton-hadron scattering is the cleanest and most precise probe of parton dynamics in protons and nuclei. The LHeC is the only current proposal for TeV-scale lepton-hadron scattering and the only medium-term potential complement to the LHC pp, AA and pA programme at the energy frontier. As such, it has a rich and diverse physics programme of its own, as documented extensively in the recent conceptual design report (CDR) [1] and summarised in an initial submission by the LHeC Study Group to the European Stratey of Particle Physics (ESPP) discussion prior to the Cracow Symposium [2]. The focus of this second submission to the ESPP is a further exploration of the relationship between the LHeC and the LHC. Specifically, by improving the understanding of the LHC initial state through tighter constraints on parton densities and providing information on many other aspects of strong interactions, the LHeC extends the capabilities of the LHC programme substantially.

The LHeC offers the prospect of synchronous operation of a new ep (and eA) facility with the GPDs in the high luminosity phase of the LHC (HL-LHC). The physics programme of the GPD experiments on this timescale, as illustrated in the ATLAS and CMS contributions to the ESPP process, is centered around two major objectives: i) the most precise and complete exploration possible of the newly discovered Higgs-like particle and ii) maximising the sensitivity of the continuing search for new particles and symmetries or extra dimensions in the few TeV range of mass. This document investigates the potential impact of precision LHeC results on these objectives, as we understand them at present, recognising that the situation will evolve with time and deserves continuous further study. It also recalls the importance of the deep inelastic electron-ion scattering for the completion of the LHC heavy ion programme. The mutual relations between the LHeC and the LHC are of course much deeper than can be covered in a brief communication such as this.

As documented in detail in [1], the parton density (PDF) determinations offered by the LHeC are substantially superior to the possibilities using LHC data alone and, for the first time, provide a full flavour decomposition essentially free of assumptions. The LHeC also promises a broad and unique programme of further strong interaction physics, such as the exploration of a newly accessed high density, low coupling regime at low x and a new level of precision and hugely extended kinematic coverage on the partonic structure of nuclei. Combined with competitive sensitivity to new physics in channels where initial state lepton quantum numbers are an advantage, the LHeC represents a cost effective means of fully exploiting the LHC and substantially extending its physics programme.

Following the discovery by ATLAS [3] and CMS [4] of a new boson with a mass of about 126 GeV, the future focus of the field will be firstly on determining whether this particle is the Standard Model Higgs boson or something more exotic and secondly on extending the sensitive range for discovery of other new particles as far as possible. ATLAS and CMS have reported exclusion limits for a wide range of massive new particles in the $1 - 2$ TeV range. With no strong evidence for new effects so far, the need to further extend such searches to the largest masses possible is paramount. The increased beam energy following LS1 will provide a first major step in this direction. Beyond that, further progress is limited by luminosity, due to the fast-falling cross sections as higher and higher x PDFs are involved (especially for gluon initiated processes), and by the uncertainities on those PDFs. To fully exploit the new particle discovery range of the LHC, both a luminosity upgrade and tighter external PDF constraints are therefore required.

The future exploration of the Higgs sector at the LHC, for example by measuring relative couplings and testing the CP structure, may similarly become limited by theory uncertainties derived from PDF measurements once the very high luminosities possible at HL-LHC have been accumulated [5]. This is particularly true for the 'working horse' channels in which the Higgs decays to $\gamma\gamma$ or four charged leptons. Whilst LHC inclusive W and Z production data will somewhat improve constraints on the quark densities of the proton at the electroweak scale, they will have a limited impact on the gluon density, which is more pertinent to Higgs physics, given the dominant gg production mechanism.

The present document is organised as follows. Section 2 presents a brief reminder of the Linac-Ring configuration of the LHeC, which is being prepared via prototype and design developments with a view to endorsement of the project in the next few years. This includes a brief exploration of possible ways of enhancing the luminosity to the level of $10^{34}\,\mathrm{cm}^{-2}\mathrm{s}^{-1}$. Section 3 is devoted to PDF determinations, including the relation between pp and ep, the LHeC's potential to unfold all quark flavours and to unfold the gluon

2

density to an unprecedented level of precision in a huge x range. Section 4 provides a discussion of two key features of the LHeC which may be crucial in the establishment of new theories or particles: the prospect of measuring α_s to per mille accuracy and the precision calculation of SUSY cross sections involving high x partons at the limits of the accessible HL-LHC mass range, gluino pair production being used as an example. Section 5 discusses the main contributions of the LHeC to Higgs physics; its potential to find new physics at the cleanly accessible WWH (and ZZH) vertices and the corresponding precision coupling measurements to vector bosons, as well as its reduction of the QCD-dominated theory uncertainties on Higgs production in pp collisions. Finally, in Section 6, the importance of eA DIS measurements for the LHC heavy ion programme is briefly reviewed.

2   The LHeC Linac-Ring Collider

The LHeC aims at colliding the high-energy protons and heavy ions circulating in the LHC with 60-GeV polarized electrons and possibly also positrons. The LHeC is realized by adding to the LHC a separate 9-km racetrack-shaped recirculating superconducting (SC) energy-recovery linac (ERL). The key components of the LHeC are the two 1-km 10-GeV SC linacs of the ERL, comparable in scale to the 17.5-GeV SC linac of the European XFEL presently under construction. The LHeC ERL provides a design lepton beam current of 6.4 mA at the ep collision point, which is taken to be at IP2 of the LHC. Aside from the IP2 interaction region, the LHeC underground infrastructure is fully decoupled from the existing LHC tunnel. Two of the access shafts could be located on the CERN Prevessin site.

The LHeC is designed to operate with simultaneous LHC pp (or AA) collisions. LHeC operation is fully transparent to the other LHC experiments thanks to the low lepton bunch charge and resulting minuscule beam-beam tune shift experienced by the protons, together with the choice of the LHeC circumference to be equal to a third of the LHC's in order to allow for ion-clearing gaps in the ERL without perturbing LHC steady-state operation.

parameter [unit]	LHeC	
species	e	p, $^{208}\text{Pb}^{82+}$
beam energy (/nucleon) [GeV]	60	7000, 2760
bunch spacing [ns]	25, 100	25, 100
bunch intensity (nucleon) [10^{10}]	0.1 (0.2), 0.4	17 (22), 2.5
beam current [mA]	6.4 (12.8)	860 (1110), 6
rms bunch length [mm]	0.6	75.5
polarization [%]	90 (e^+ none)	none, none
normalized rms emittance [μm]	50	3.75 (2.0), 1.5
geometric rms emittance [nm]	0.43	0.50 (0.31)
IP beta function $\beta^*_{x,y}$ [m]	0.12 (0.032)	0.1 (0.05)
IP spot size [μm]	7.2 (3.7)	7.2 (3.7)
synchrotron tune Q_s	—	1.9×10^{-3}
hadron beam-beam parameter	0.0001 (0.0002)	
lepton disruption parameter D	6 (30)	
crossing angle	0 (detector-integrated dipole)	
hourglass reduction factor H_{hg}	0.91 (0.67)	
pinch enhancement factor H_D	1.35 (0.3 for e^+)	
CM energy [TeV]	1.3, 0.81	
luminosity / nucleon [10^{33} cm^{-2}s^{-1}]	1 (10), 0.2	

Table 1: LHeC parameters. The numbers give the default values with optimum values for maximum ep luminosity in paranthesis and values for the ePb configuration separated by a komma.

LHeC has been designed under the constraint that the total electrical power for the LHeC lepton branch

should not exceed 100 MW (about half the present maximum CERN site power). The LHeC electrical power budget is dominated by the RF and by the cryo power for the two 1-km long SC linacs. The cryo power required and, therefore, also the size of the cryoplants (as well as the maximum lepton current) are directly linked to the unloaded quality factor of the cavities, Q_0. With a Q_0 of 2.5×10^{10}, the total main-linac cryopower amounts to 23 MW. The RF power needed for RF microphonics control is about 24 MW, and the extra-RF power needed for compensating SR losses at 6.4-mA current also to 23 MW. The remaining components, like injectors or arc magnets, require a few MW each.

Together with rather conservative assumptions for most parameters, the 100 MW power limit yields the LHeC ep target luminosity of 10^{33} cm^{-2}s^{-1}. However, extensions to significantly higher luminosity, e.g., 10^{34} cm^{-2}s^{-1}, are possible by a combination of improvements, namely (1) by considering a normalized proton beam emittances of 2 μm (as achieved in 2011/12 LHC operation) instead of 3.75 μm; (2) by a further reduction of the proton IP beta function from 0.1 m down to 0.05 m, which should be possible by using a variant of the so called ATS optics; (3) by increasing the proton bunch intensity from 1.7×10^{11} to the HL-LHC 25 ns target value of 2.2×10^{11} [for the 50-ns HL-LHC scenario it would be even 3.3×10^{11} with a possible further factor 2.5 increase of luminosity, to more than 2×10^{34} cm^{-2}s^{-1}]; and (4) by doubling the lepton beam current, which should be possible without exceeding the 100-MW power limit if the unloaded Q_0 value of the SC RF cavities can be raised to 4×10^{10} (as it is assumed for the similar eRHIC design). Table 1 shows LHeC parameters, including, in parentheses, values for a higher-luminosity variant.

The LHeC represents an interesting possibility for further efficient exploitation of the LHC infrastructure investment. The development of a CW SC recirculating energy-recovery linac for LHeC would prepare for many possible future projects, e.g., for an International Linear Collider, for a neutrino factory, for a proton-driven plasma wake field accelerator, or for a muon collider. With some additional arcs, using 4 instead of 3 passes through the linacs, a machine like the LHeC ERL (without energy recovery) could also operate as a Higgs factory $\gamma\gamma$ collider (SAPPHiRE).

3   Parton Distributions

3.1   PDFs in pp and ep

The factorization theorems of perturbative QCD (see Ref. [6] and references therein) express physical observables for hard processes characterized by a large momentum scale as the convolution of a perturbatively computable partonic cross-section, determined in terms of the degrees of freedom of the QCD Lagrangian — quarks and gluons — and universal, process–independent parton distributions, up to corrections suppressed by powers of the ratio of a characteristic QCD scale $\Lambda \sim 100$ MeV to the large scale.

Factorization is most rigorously established for deep inelastic lepton-hadron scattering, where the expression for the cross-section has schematically the form

$$\sigma_{DIS}(x, Q^2) = \int_x^1 \frac{dz}{z} \, \hat{\sigma}_{DIS}(z, \alpha_s(Q^2)) f\left(Q^2, \frac{x}{z}\right), \tag{1}$$

where $\sigma_{DIS}(x, Q^2)$ denotes generically a deep inelastic structure function, Q^2 is the hard scale of the process, namely, the virtuality of the gauge boson which mediates the scattering process, and the scaling variable is $x = Q^2/2p \cdot q$ in terms of the incoming hadron momentum p and momentum transfer $q = k' - k$ between the incoming (k) and outgoing (k') lepton momenta. In Eq. (1), the partonic cross section $\hat{\sigma}_{DIS}(z, \alpha_s(Q^2))$ can be computed as a perturbative expansion in $\alpha_s(Q^2)$, while $f\left(Q^2, x\right)$ is a parton distribution; a sum over different kinds of partons (individual quark flavours and gluons) is understood but omitted for simplicity. Equation (1) directly follows from the Operator-Product Expansion, though it can also be derived from the computation of parton Feynman diagrams.

Factorization for hadronic cross-sections, such as for example the production of an electroweak final state such as a Higgs or a W or Z takes the form

$$\sigma_{DY}(\tau, M^2) = \int_\tau^1 \frac{dz}{z} \, \hat{\sigma}_{DY}(z, \alpha_s(M^2)) \mathcal{L}\left(\frac{\tau}{z}\right), \tag{2}$$

4

where now $\sigma_{DY}(\tau, M^2)$ and $\hat{\sigma}_{DY}(z, \alpha_s(M^2))$ are respectively hadronic and partonic cross sections for production of the electroweak final state of mass M: with the hadronic σ measurable, and the partonic $\hat{\sigma}$ computable in perturbation theory, and the scaling variable is $\tau = \frac{M^2}{s}$. The dependence on parton distributions now goes through the parton luminosity

$$\mathcal{L}(\tau) = \sum_{a,b} \int_\tau^1 \frac{dx}{x} f_{a/h_1}(x) f_{b/h_2}(\tau/x), \tag{3}$$

which depends on the parton distribution from parton a and b, respectively, extracted from the two incoming hadrons h_1 and h_2. Again, we have neglected a sum over partonic channels for simplicity.

Because taking a Mellin transform turns the convolutions in Eqs.(1-2) into ordinary products, the universality of PDFs implies that one can form a PDF-independent measurable ratio:

$$\frac{\sigma_{DY}(N, M^2)}{\sigma_{DIS}^2(N, M^2)} = \frac{\hat{\sigma}_{DY}(N, M^2)}{\hat{\sigma}_{DIS}^2(N, M^2)}, \tag{4}$$

where $\sigma_{DY}(N, M^2) = \int_0^1 d\tau \, \tau^{N-1} \sigma(\tau, M^2)$, and analogously for the other cross sections. It is the possibility of constructing such a ratio, which only depends on perturbatively computable partonic cross sections, which guarantees predictivity of Drell-Yan processes for example.

Factorization for hadronic processes in which a colorless electroweak final state is produced, such as Higgs, or a real or virtual W, Z or γ is firmly established on the basis of an all-order analysis of the relevant Feynman diagrams. Furthermore, such processes are currently available up to NNLO in perturbation theory at the differential level and partly at N^3LO for total cross sections: no counterexample to factorization has been found up to this order. Factorization is also well-established for sufficiently inclusive colored final states, such as the one-jet and dijet cross section. In this case no fully rigorous all-order argument is really available, but no counterexample to factorization has ever been found either.

Recent global determinations of parton distributions, such as CTEQ [7], MSTW [8] or NNPDF [9] combine both deep inelastic scattering data with a variety of beams (electrons, muons, neutrinos) and targets (protons, deuterons and heavier nuclei) as well as hadron-hadron data such as virtual photon (Drell-Yan) production, W and Z production, and single jet production. A typical such analysis includes over 2000 deep inelastic data points, and over 1000 hadronic data points. It thereby provides both a test of the factorization framework which guarantees the mutual consistency of these data, and a possibility of assessing their relative impact.
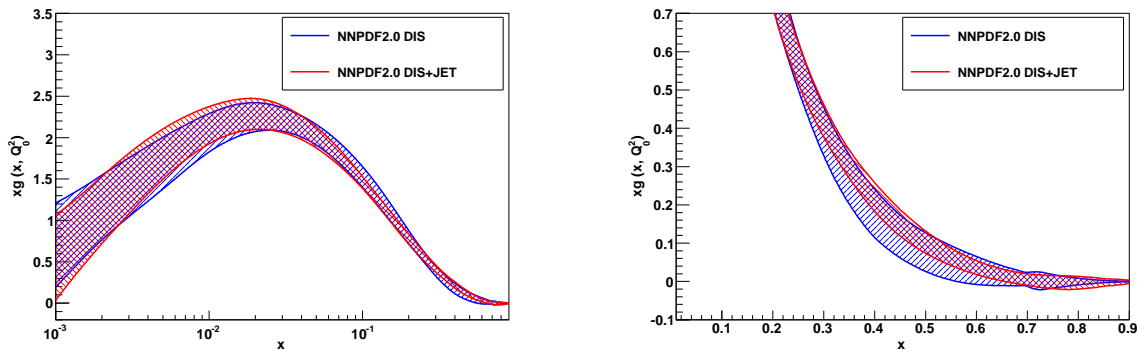

Figure 1: The gluon distribution determined using deep inelastic scattering data only (blue) or also including jet data (red), plotted on a logarithmic (left) and linear (right) scale vs x at $Q^2 = 2$ GeV^2 (from [10]).

As an example of both, Figure 1 compares the gluon distribution extracted by only fitting deep inelastic scattering data, and by also adding jet data to the DIS dataset. Such a comparison provides an interesting

test of factorization for at least three reasons. First, because one is comparing a lepton-hadron and a hadron-hadron process. Second, because the gluon is determined through rather different physical mechanisms: in deep inelastic scattering, where it does not couple to the leading-order perturbative process because it carries no electric or weak charge, the gluon is determined by the Q^2 evolution. In jet production, instead, it directly contributes both to the initial and final state. Finally, because the jet data are taken at scales which are typically one or two orders of magnitude larger than that of the deep inelastic data, and thus the parton distribution extracted from one process has to be evolved through renormalization group equations in order to be used in the other process. Nevertheless, it is apparent from Fig. 1 that the gluon determined by deep inelastic scattering and jets is consistent: when adding jet to deep inelastic data, the central value moves very little, while the uncertainty is somewhat reduced. It is also apparent from the figure that the bulk of the information on the gluon distribution is coming from deep inelastic scattering, with the jet data only providing some useful but no determinant extra information.

Both these situations are generic, and likely to persist in the future. On the one hand, perturbative factorization is now firmly extablished for a variety of processes, and electron-proton data can thus reliably provide input for hadron collider processes. In fact, because factorization is most reliably established in deep inelastic scattering, it is the availability of precise parton distributions from lepton-hadron scattering which may allow detailed tests of the validity of factorization for processes for which it is less established. On the other hand, because lepton-hadron data are generally subject to smaller power-suppressed corrections, perturbatively more stable, easier to compute than most hadronic processes so results to the highest pertiurbative orders are available, and finally free of many complications which arise when dealing with hadronic initial and final states (such as jet definitions, or underlying event), lepton-proton data always provide comparatively more competitive and theoretically reliable determination of parton distributions than hadron-hadron data. The natural scenario is one in which lepton-proton data are used to determine parton distributions, and the latter are then used for hadron collider processes, and there are strong reasons of principle why this is the case.

3.2   NC and CC Cross Section Measurements

The determinations of parton distributions at the LHeC are of unique range and quality because of a number of salient features which characterise this experiment, especially with respect to HERA: i) The LHeC greatly extends the kinematic range compared to HERA. The increase in negative momentum transfer squared Q^2 is from a maximum of about 0.03 at HERA to $1\,\mathrm{TeV}^2$ at the LHeC, and in x, e.g. for $Q^2 = 3\,\mathrm{GeV}^2$, from about $4 \cdot 10^{-5}$ to $2 \cdot 10^{-6}$. ii) The projected increase of integrated luminosity by a factor of 100 allows to also extend the kinematic range at large x, from practically about 0.4 to 0.8 in charged currents (CC). This enables a precision mapping of the high x region, corresponding to large masses, of a few TeV, in Drell-Yan scattering at the LHC. iii) The increase in Q^2 implies that all parts of the neutral current cross section, due to pure photon and pure Z exchange, and their interference become of equal strength. This, combined with high precision and CC data in a large kinematic range, enables a complete separation of sea and valence quarks. It is crucial to understand that such a basis of PDF determinations will render all previous PDF determinations of inferior importance and practically reduce any parameterisation uncertainty in QCD PDF fits to a negligible level of importance.

The superior nature of the DIS process for testing partons, with respect to Drell-Yan scattering, the higher precision in ep wrt pp and the availability of an enormous range in Q^2 for fixing parton evolution, as opposed to the $Q^2 \simeq M^2_{W,Z}$ scale of the most accurate DY process at the LHC, these and further features make the LHeC the appropriate machine for transforming the LHC into a precision QCD, search and Higgs factory in the twenties.

The analysis of PDF measurements of the LHeC has been based on a full simulation of the NC and CC inclusive cross section measurements. The assumptions on sources of systematic uncertainty are listed in Table 2 [1]. Broadly speaking, it is assumed that with a new detector and high luminosity the H1 level of systematic uncertainty is reached and improved by up to a factor of two. The measurements of PDFs at the LHeC are complemented by high precision measurements of the heavy flavour quark densities owing to a small beam spot, high luminosity and modern Silicon tracking techniques of high precision and wide acceptance.

source of uncertainty	error on the source or cross section
scattered electron energy scale $\Delta E'_e/E'_e$	0.1 %
scattered electron polar angle	0.1 mrad
hadronic energy scale $\Delta E_h/E_h$	0.5 %
calorimeter noise (only $y < 0.01$)	1-3 %
radiative corrections	0.5%
photoproduction background (only $y > 0.5$)	1 %
global efficiency error	0.7 %

Table 2: Assumptions used in the simulation of the NC cross sections on the size of uncertainties from various sources. These assumptions correspond to typical best values achieved in the H1 experiment. The total cross section error due to these uncertainties, e.g. for $Q^2 = 100\,\mathrm{GeV}^2$, is about 1.2, 0.7 and 2.0 % for $y = 0.84,\ 0.1,\ 0.004$.

An important part of the PDF programme at the LHeC is due to the projected run with deuterons, which extends the knowledge of neutron structure from DIS by 4 orders of magnitude in kinematic range. It needs deuterons to measure a singlet combination of parton densities and to unfold the light sea flavour composition at low x. The LHeC is also an ideal and necessary configuration to determine the nuclear PDFs for the first time in most of the kinematic range as is emphasised below.

3.3 Valence and Sea Quarks

The LHeC is in a unique position to unravel all quark densities in the proton with a complete quark flavour separation for the first time and with unprecented precision. The huge phase space covered matches the needs of the LHC and includes the extreme values of Bjorken x, lowest, $x \simeq 10^{-5}$, where saturation may set in and largest, near to 1, which determine the multi-TeV BSM cross sections at the LHC. The detailed shape measurements of the various parton distributions, for example of the strange density versus Q^2 and x, imply that the nowadays large uncertainties due to PDF parameterisations in pQCD fits will be drastically reduced. A complete base of PDFs as the LHeC promises to deliver will at many places lead to possibly sizeable deviations of the now canonical PDF pattern. This is a necessary input for future LHC measurements, as precision *Higgs* coupling and cross section determinations. There are also expectations that discoveries are made in the conventional PDF pattern, as by possible observations of anti-quarks to be different from their sea quarks or an intrinsic heavy flavour part. Since the momentum is conserved, and shared between quarks and gluons, any deviation affects the overall pattern, which reflects on other parts of physics [2]. Moreover, a crucial variety of non-canonical PDFs will be accessed: generalised, unintegrated, diffractive, neutron, photon and nuclear parton distributions.

The basis of LHC physics and discoveries BSM is QCD at high orders and the accurate knowledge of the classic PDFs. In the following, based on [1], some brief remarks are made on the unique potential of the LHeC in the determination of the complete set of quark densities, while the mapping of the gluon density is described subsequently below.

- **Valence quarks:** The knowledge of the valence quark distributions, both at large and at low Bjorken x, as derived in the current world data QCD fit analyses is amazingly limited. An impressive improvement is expected from the LHeC. A NLO QCD fit to simulated inclusive neutral and charged current LHeC data (see [1]) shows that the uncertainty of the down valence quark distribution at, for example, $x = 0.7$ can be reduced from a level of $50 - 100\,\%$ to about 5 %. This will be crucial for searches of new physics at the LHC at the high energy frontier, in order to verify any excess (or deficiency) compared to the SM prediction. Direct access to valence quarks down to low $x \sim 0.001$ can be obtained at LHeC

---

[2] A recent example is the ATLAS observation of the light sea to be flavour symmetric. Combined with the precision HERA F_2 data this changes the singlet sea by 8 %, which has consequences for the ultra high energy neutrino-nucleon scattering cross sections.

from the NC, Z exchange related $e^{\pm}p$ cross section difference, which can resolve possible sea-antiquark differences.

- **Light sea quarks:** The measurement of the structure functions $F_2 \propto 4U + D$, in ep and $F_2 \propto U + D$, in eD is the basis for determining the light sea quark densities in the nucleon. LHeC will extend greatly the HERA kinematic coverage to much lower x and to higher scales Q^2. From NC and CC measurements and comparing ep with eD data, the up and down sea quark densities will be unfolded, which nowadays are assumed to be equal at $x < 0.01$.

- **Strange:** Several long-standing questions are related to the strange quark density in the proton: how much is it suppressed with respect to the other two light quarks? Is there an asymmetry between the strange and anti-strange density? The knowledge of the strange-quark density itself is important for many processes, for instance for the precision measurement of the W boson mass. Information on the strange quark density is available from several experiments, in particular from previous Neutrino DIS experiments[3], but overall there is no real understanding of the strange quark distribution. The strange quark distribution is accessible at LHeC in charged current scattering through the subprocesses $W^+ s \to c$ (for positron beams) and $W^- \bar{s} \to \bar{c}$ (for electron beams), with charm tagging in the final state. The LHeC simulation studies show that for the first time accurate measurements of the s and $\bar{s}$ densities can be performed over a large kinematical phase space in x and Q^2.

- **Charm:** Information on the charm content in the proton can be accessed at LHeC by measuring the inclusive charm production cross section in neutral current DIS. At low scales $Q^2 \sim m_c^2$ (with m_c being the charm quark mass) one has to treat the charm production fully massive, i.e. the charm quarks can be only dynamically produced in the reaction $\gamma g \to c\bar{c}$ and thus are themselves no active flavours in the proton. However, at large scales $Q^2 \gg m_c^2$ one can treat the charm quarks as massless partons, which are contributing to the sea. The charm quark mass m_c is a crucial parameter: it regulates the ratio of charm and light quarks in the sea and thus affects predictions for almost any quark driven process at the LHC. At LHeC one expects much more precise and kinematically extended measurements of inclusive charm production compared to HERA. This will allow to map for the first time the transition from the massive to the massless regime. Simulations show that one can use the data for a m_c determination at a precision of two permille. With very good forward charm tagging one can also test the hypothesis of an intrinsic charm component in the proton wave function, which could appear at high $x \simeq 0.2$.

- **Beauty:** Simulation studies show that one expects at LHeC precise measurements of inclusive beauty production in DIS. For large squared momentum transfer $Q^2 \gg m_b^2$ (with m_b being the beauty quark mass) these measurements can be directly translated into an effective beauty quark density in the proton. There is a huge interest in these densities, since in many scenarios of new physics the beauty quarks are the original particles. For instance in the minimal supersymmetric extension of the standard model the production of the neutral Higgs boson A is driven by $b\bar{b} \to A$. While at HERA the inclusive beauty production results were statistically limited to about 20% precision, very accurate results can be expected at the LHeC.

- **Top:** The production of top quarks can be studied at the LHeC for the first time in DIS experiments. The dominant process is single top (or anti-top) production in Wb to t fusion. The unique top physics program that can be performed at the LHeC includes possibly the consideration of a quark density for the top, from NC, a high precision measurement of the top mass from its decay and cross section. Top physics at the LHeC is a promising subject for further study.

In summary, while the LHC data can add information to certain aspects of the quark densities in the proton using specific reactions (e.g. Drell Yan), it remains reserved for the LHeC to uniquely resolve the complete quark and antiquark structure of the proton, for all quark flavours, over the largest kinematic range ever and last but not least with the best theoretical understanding.

---

[3]The interpretation of these neutrino data is sensitive to uncertainties from charm quark fragmentation and nuclear corrections.

3.4 Gluon Distribution

As has been summarised in the CDR, there are many fundamental reasons for the necessity to understand the gluon distribution and the gluon-parton interactions deeper than hitherto. Half of proton's momentum is carried by gluons. Gluon self-interaction is responsible for the creation of baryonic mass. In pp scattering at the LHC, the Higgs particle is predominantly produced by gluon-gluon interactions. Gluino pair production, as discussed in Section 4.2, predominantly proceeds via $gg \rightarrow g \rightarrow \tilde{g}\tilde{g}$ production and is hugely uncertain at high masses. On the other hand the rise of the gluon density towards low Bjorken $x \lesssim 10^{-5}$ is expected to be tamed and a new phase of hadronic matter to be discovered, in which gluons interact non-linearly while α_s is smaller than 1.
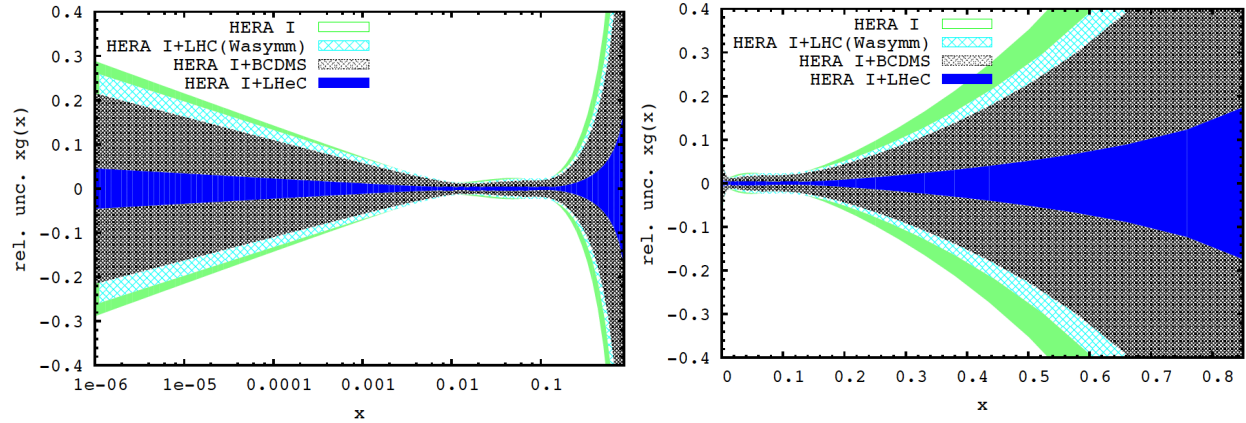

Figure 2: Relative uncertainty of the gluon distribution at $Q^2 = 1.9\,\mathrm{GeV}^2$, as resulting from an NLO QCD fit to HERA (I) alone (green, outer), HERA and BCDMS (crossed), HERA and LHC (light blue, crossed) and the LHeC added (blue, dark). Left: logarithmic x scale, right: linear x scale.

From the simulations as described one derives a typical uncertainty for the gluon density to be reduced to about 3, 1, 5 % at $x = 5 \cdot 10^{-6}$, 0.005, 0.5, respectively. These values of Bjorken x mark the low value for saturation to be discovered, the central rapidity value for Higgs production and about the high mass limit for gluino pair production. Obviously, see Figure 2, the potential of the LHC for the determination of the gluon density over $5 - 6$ orders of magnitude in x, simultaneously with all quark PDFs and α_s, is striking. It has to be compared with the current status of huge uncertainty on xg at low and high x as is illustrated in Figure 3.

4 PDFs for BSM Searches

4.1 Strong Coupling and Grand Unification

Deep inelastic scattering is an ideal process for the determination of the strong coupling constant, which determines the scaling violations of the parton distributions. Despite a major effort for the past more than 30 years, there is no precise determination of α_s available, of a precision competing with QED or weak couplings, and a number of severe questions remains to be solved as is discussed in [1] and has recently been summarised in [11]. Questions regard the (in)consistency of previous DIS data, the (in)consistency of inclusive DIS and jet based data, the true uncertainty of the world average on α_s including the role of various lattice QCD determinations etc. It is for these reasons and because of the importance of α_s for the grand unification of gauge theories as for a plethora of predictions of cross sections, as of Higgs production at the LHC, that an experimental determination of the strong coupling with an order of magnitude improved precision is crucial. It is also time to challenge the lattice QCD α_s results, which seem to be most accurate
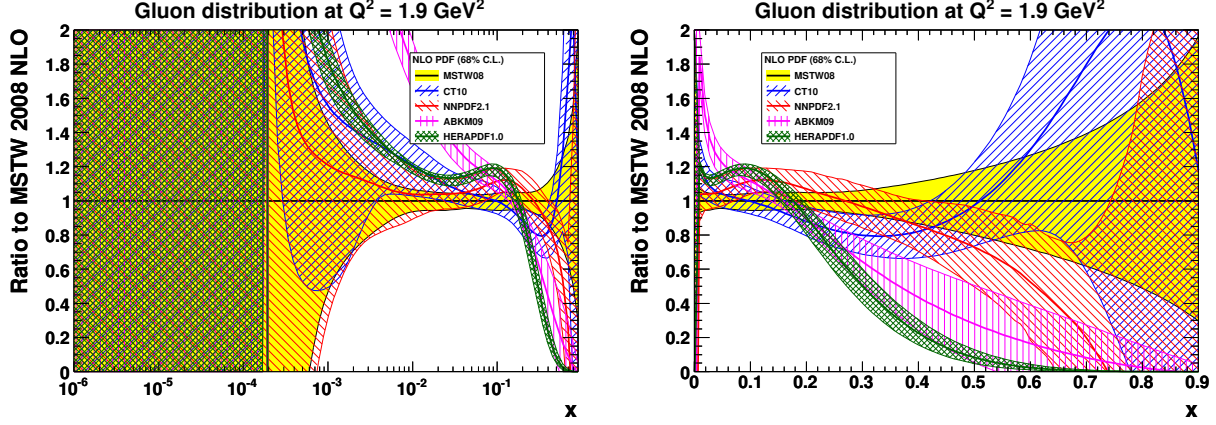
Figure 3: Ratios to MSTW08 of gluon distribution and uncertainty bands, at $Q^2 = 1.9\,\mathrm{GeV}^2$, for most of the available recent PDF determinations, taken from [1]. Left: logarithmic x scale, right: linear x scale.

case	cut $[Q^2\ (\mathrm{GeV}^2)]$	uncertainty	relative precision (%)
HERA only	$Q^2 > 3.5$	0.00224	1.94
HERA+jets	$Q^2 > 3.5$	0.00099	0.82
LHeC only	$Q^2 > 3.5$	0.00020	0.17
LHeC+HERA	$Q^2 > 3.5$	0.00013	0.11
LHeC+HERA	$Q^2 > 7.0$	0.00024	0.20
LHeC+HERA	$Q^2 > 10.$	0.00030	0.26

Table 3: Results of NLO QCD fits to HERA data (top, without and with jets) to the simulated LHeC data alone and to their combination, for details of the fit see [1]. The resulting uncertainty includes all the statistical and experimental systematic error sources taking their correlations into account.

but which exhibit variations which are non-negligible [11].

Two independent simulations and fit approaches have been undertaken in order to verify the potential of the LHeC to determine α_s, see the CDR [1] for details. Table 3 summarises the main results. It can be seen that the total experimental uncertainty on α_s is 0.2 % from the LHeC and 0.1 % when combined with HERA. This determination is free of higher twist, hadronic and nuclear corrections relying solely on inclusive DIS ep data at high Q^2. There are known further parametric uncertainties in DIS determinations of α_s. These can safely be expected to be much reduced also by the LHeC, which promises to determine the charm mass, for example, by 3 MeV, as compared to 30 MeV at HERA, corresponding to an α_s uncertainty of 0.04 %. Matching the experimental uncertainty requires that when the LHeC operates such analyses were performed in N^{3}LO pQCD in order to reduce the scale uncertainty. The ambition to measure α_s to per mille accuracy therefore represents a vision for a renaissance of the physics of deep inelastic scattering which is a major goal of the whole LHeC enterprise. Due to the huge range in Q^2 and the high precision of the data new, decisive tests will also become available for answering the question whether the strong coupling determined with jets and in inclusive DIS are the same. If confirmed, as is demonstrated in Table 3 with the HERA data, a joint inclusive and jet analysis has the potential to even further reduce the uncertainty of α_s as simulated here.

Numerous tests of the running of α_s have been performed. At even higher scales, the law which governs this behaviour would be affected, possible strongly as is illustrated in Figure 4 (left), if extra dimensions showed up in the kinematic range accessible to the LHeC. Besides effects on α_s one would expect to see changes of the NC cross section, as in contact interaction patterns, for which the LHeC provides a range up to about 50 TeV, which is discussed in the CDR.
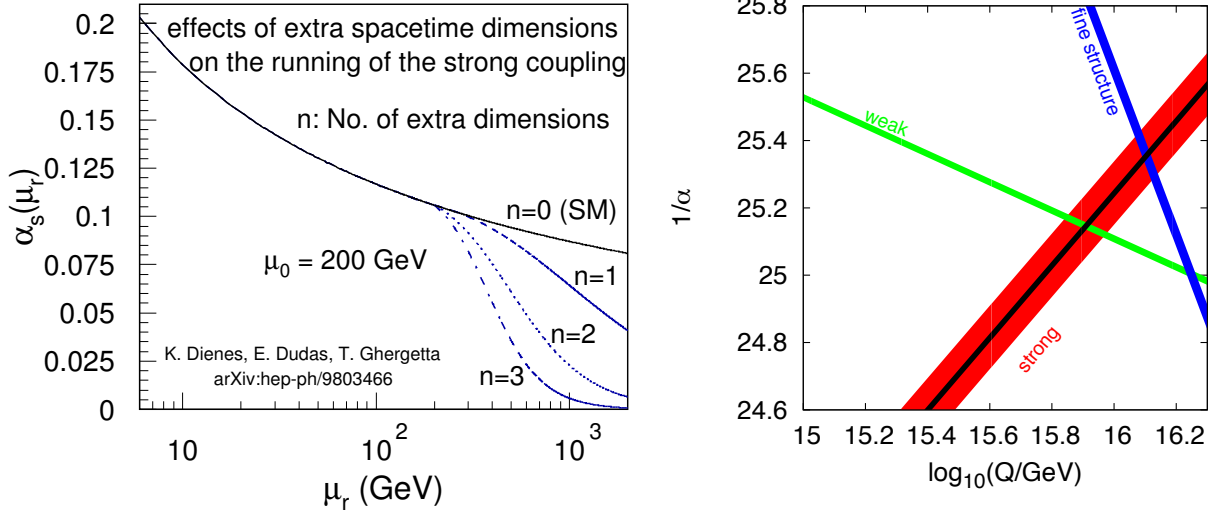
10

Figure 4: Left: Running of the strong coupling constant up to high scales $\sqrt{Q^2} = \mu$ in the absence (SM) and presence of n extra dimensions [12]; Right: Extrapolation of the coupling constants ($1/\alpha$) within the MSSM (for the parameter point CMSSM40.2.5 [13]) to the Grand Unified scale as predicted by SOFTSUSY [14]. The width of the red line is the uncertainty of the world average of α_s, which is dominated by the lattice QCD calculation chosen for the PDG average. The black band is the LHeC projected experimental uncertainty [1].

It is well known that grand unified theories (GUTs), having only a single gauge group, thus possess a single gauge coupling of that group. The Standard Model (SM) gauge couplings are derived, after spontaneous breaking of the GUT, from the renormalisation group evolution of the gauge couplings, from the Grand Unified scale to the weak scale where they are measured. Thus there is a testable GUT prediction: the couplings, which are measured at about the weak scale, should all unify to a common value at a single, very high energy scale. Assuming the SM as the relevant effective field theory, they do not unify. However, assuming a supersymmetric desert above the weak scale and using the minimal supersymmetric standard model (MSSM), the strong and electroweak couplings do approximately unify at a common scale of $M_{GUT} \approx 2 \cdot 10^{16}$ GeV. In the specific calculation used here, the couplings do not quite match, see Figure 4 (right). In realistic GUTs such deviations may occur and are caused by threshold effects, for example by the prediction of heavy GUT relic particles that lie just below M_{GUT}. An accurate inference of this deviation therefore gives important clues into the structure of such heavy states and therefore, ultimately, the GUT itself. It is visible that the present level of uncertainty of the strong coupling is much larger than that of the weak coupling and the fine structure constant, while with the LHeC a huge improvement is expected.

4.2 Supersymmetry

Supersymmetry (SUSY) is a compelling theory providing an extension of the Standard Model (SM) at high energies. In the SM, the Higgs boson mass suffers from large quantum loop corrections, as large as the cut-off scale of the theory, and therefore needs a high degree of fine-tuning of parameters to be cancelled. With SUSY, this 'naturalness problem' is solved by the addition of supersymmetric partner particles to the known fermions and bosons which cancels the largest of these loop effects and permits the Higgs boson mass to lie naturally at the ~ 100 GeV scale. Supersymmetric theories present other advantages, including the unification of running coupling constants at the Planck scale, see Sect. 4.1, and renormalization group equations that radiatively generate the scalar potential that leads to electroweak symmetry breaking. Yet, at the LHC there is so far no sign for SUSY particles. It therefore is crucial to enlarge the beam energy and luminosity to extend these searches to the limit of phase space.

11

The possible (non)conservation of the discrete R-parity, which relates spin (S), baryon and lepton numbers (B and L), is fundamental to determine the SUSY phenomenology. In the framework of a generic R-parity conserving supersymmetric extension of the SM, SUSY particles are produced in pairs and the lightest supersymmetric particle (LSP) is stable. In a large variety of models the LSP is the lightest neutralino, $\tilde{\chi}_1^0$, one of the SUSY partners of the gauge bosons together with its three heavier mass eigenstates ($\tilde{\chi}_{2,3,4}^0$) and the charginos ($\tilde{\chi}_{1,2}^\pm$). The lightest neutralino only interacts weakly and provides a Dark Matter candidate with the appropriate relic density to possibly explain the cosmological Dark Matter.

The possible appearance of R-parity-violating couplings, and hence the non-conservation of baryon and lepton numbers (B and L) in supersymmetric reactions, imply an even richer phenomenology. Although R-parity-violating interactions must be sufficiently small, a most dramatic implication of interactions from R-parity violations is the automatic generation of neutrino masses and mixings. The possibility that the results of atmospheric and solar neutrino experiments may be explained by neutrino masses and mixings originating from R-parity-violating interactions has thus motivated a large number of studies and models.

The discovery (or exclusion) of supersymmetric particles remains a prime priority for the LHC experiments which search for physics beyond the SM at the TeV scale. At the LHeC, SUSY particles could be produced due to sizable lepton flavour violating terms or, in the framework of R-parity conserving models, via associated production of selectrons and first and second generation squarks. The latter process would present a sizable cross section only if the sum of selectron and squark masses is below or around 1 TeV, i.e. for relatively light squarks. Current exclusion limits set by the ATLAS and CMS experiments on first and second generation squarks extend up to $\simeq 1.5\,\mathrm{TeV}$, under the assumption that the first two squark families are degenerate. In models where this condition is relaxed, windows of discovery relevant for the LHeC might still be open at the time of start-up.

Less stringent constraints exist in the context of R-parity violating scenarios. Processes of interest for the LHeC include leptoquark-like processes and associated production of quark-neutralinos via squark-quark-neutralino couplings, where squarks can be off-shell and thus beyond direct LHC exclusion limits. While stringent constraints exist for associated production of leptons and quarks possibly deriving from squark decay, processes of the kind $eu \to d\tilde{\chi}_1^0$ and subsequent decays of $\tilde{\chi}_1^0$ to leptons and quarks might be difficult to study at the LHC, due to the overwhelming SM multi-jet background, and be succesfully searched for at the LHeC. The LHeC will also provide indirect handles for the case of supersymmetry.

The dominant SUSY production channels at the LHC are assumed to be squark-(anti)squark, squark-gluino, and gluino-gluino pair production. All gluon-initiated processes suffer from very large uncertainties due to the highly limited knowledge of the gluon density at high x. If gluinos of $2-4\,\mathrm{TeV}$ mass exist, their discovery and kinematic characterisation will depend on the capability to predict their production cross section with good precision.

Fig. 5 shows the amount of PDF uncertainties, current and expected, on the gluino-pair production cross section calculated at NLO SUSY-QCD expressed as the ratio to the MSTW08 predictions. The cross section calculation is based on [15] and assumes that first and second generation squarks are mass degenerate and equivalent to the gluino mass. The renormalization and factorization scale is set to the squark/gluino mass. Several of the current PDF fits are considered and suffer from very large uncertainties. They also differ considerably, by factors, in their central predictions, which has to do with the smallness of the gluon distribution at large Bjorken x and the uncertainty of jet physics constraints at the Tevatron and the LHC, related to scale and calibration uncertainties and to the size of theory corrections at high mass Drell-Yan scattering. On the other hand, predictions employing the LHeC-derived PDF fits exhibit much smaller uncertainties, between 5% and 20% for gluino masses between 500 GeV and 5 TeV, thanks to the expected precision LHeC measurements of the NC and CC cross sections, and the derived quark and gluon densities, see above and [1].

Such a greatly reduced level of uncertainty is comparable or below the experimental uncertainties expected for squark/gluino searches at the high-luminosity LHC, e.g. through enhanced multi-jet production rates (with or without missing transverse momentum) compared with SM predictions. It is difficult to predict the fate of high mass searches for SUSY. However, it is a prime goal of the GPD LHC experiments in the HL-LHC phase to explore the phase space to the or close to the kinematic limit. Fig. 5 makes it clear that
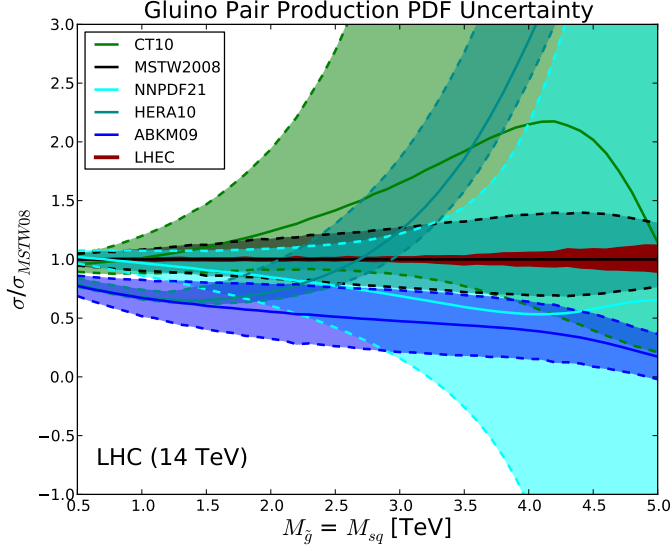
Figure 5: Calculation of gluino pair production in NLO SUSY-QCD using Prospino [16] and assuming squark mass degeneracy and equality of squark and gluino masses for illustration. The error bands are around central values (solid lines) and correspond to the uncertainty quotations of the various PDF groups. The red band of uncertainty for the LHeC corresponds to the statistical and systematic errors including their correlations as treated in the NLO QCD fit described in the CDR.

the exploration of the region of above a few TeV gluino mass requires to much improve the PDF, especially the gluon uncertainty for which the LHeC is the most reliable and most precise base, as has been argued above. Should deviations from SM predictions be observed, accurate predictions for inclusive squark and gluino production cross sections will be crucial to understand the nature of the new physics discovered and to determine SUSY particle masses and properties [17]. In this regard the LHeC, as an ultra-precision QCD instrument, is a necessary complement for the HL-LHC physics programme, both for high mass searches as exemplified here and for making the LHC a precision Higgs factory as will be illustrated below.

The interest in R-parity violating SUSY translates directly into the striking potential of the LHeC to determine the lepto-quark or lepto-gluon quantum numbers should such states be discovered at the LHC. The ep machine has a clean s-channel single production mode, with variable input beam parameters while the LHC produces them predominantly in pairs. This is discussed in detail in [1], as is also the reach in contact interactions, excited leptons, anomalous lepton-quark interactions and other BSM topics.

5 Higgs Measurements

In the Standard Model, the breaking of the electroweak $SU(2)_L \times U(1)_Y$ symmetry gives mass to the electroweak gauge bosons via the Brout-Englert-Higgs mechanism, while the fermions obtain their mass via Yukawa couplings with a scalar Higgs field. With the observation of a Higgs-like boson by the ATLAS [3] and CMS [4] collaborations with a mass around 126 GeV, a new research field has opened in particle physics. The measurement of the couplings of the newly found boson to the known fundamental particles will be a crucial test of the SM and a window of opportunity to establish physics beyond the SM.

At the LHeC, a light Higgs boson could be uniquely produced and cleanly reconstructed either via HZZ coupling in neutral current DIS or via HWW coupling in charged current DIS. Those vector boson fusion processes have sizeable cross sections, O(100) fb for 126 GeV mass, and they can be easily distinguished, which is a unique advantage in comparison to the VBF Higgs production in pp scattering. The observability of the Higgs boson signal at the LHeC was investigated in the CDR [1] using initially the dominant production and decay mode, i.e. the CC reaction $e^- p \to H(\to b\bar{b}) + \nu + X$, for the nominal 7 TeV LHC proton beam

13

and electron beam energies of 60 and 150 GeV. Simple and robust cuts are identified and found to reject effectively e.g. the dominant single-top background, providing an excellent S/B ratio of about 1 at the LHeC, which may be further refined using sophisticated neural network techniques. At the default electron beam energy of 60 GeV, for 80 % e^- polarisation and an integrated luminosity of 100 fb^{-1}, the Hbb coupling is estimated to be measurable with a statistical precision of about 4 %, which is not far from the current theoretical uncertainty. Typical coupling measurements, as for $\gamma\gamma$ or $4l$, are of about 10 % precision with the HL-LHC, while the specific $b\bar{b}$ coupling will be particularly difficult to measure due to high combinatorial backgrounds in pp.

The LHC is said to be inferior to a linear collider in its coupling measurement prospects. Part of this statement comes from large uncertainties, which are related to the imperfect knowledge of the PDFs and theory parameters. The LHeC, with its high precision PDF and QCD programme, will render many of these uncertainties unimportant. Currently, for example, an uncertainty of the $H \to \gamma\gamma$ cross section due to PDFs is quoted of nearly 10 % [18], based on the variation of the cross section predictions from different PDFs. This will be very much reduced with the LHeC: an iHix calculation of the NLO Higgs cross section for MSTW08, NNPDF2.3 and HERAPDF1.5 leads to intrinsic uncertainties of 1.7, 1.2 and 2.2 %, respectively, with a maximum deviation of 6.9 %. The full experimental LHeC uncertainty, however, is 0.2 %. The main advantage will be that the precision LHeC data, possibly combined with HERA, will replace essentially all previous data sets and thus lead to a much better agreement between various PDF determinations, besides the huge reduction in uncertainty with the LHeC.

A sizeable uncertainty is also related to the strong coupling constant, a difference in α_s of ± 0.005 corresponding to an about 10 % cross section uncertainty, see e.g. [19] or [20]. Obviously, the large improvement in the determination of α_s with the LHeC will reduce this uncertainty strongly too. Essentially with such a high quality data set as the LHeC, one will simultaneously determine the coupling and the PDFs, and control their correlations at a very high level. In [21] a systematic evaluation has been presented of the effect of the heavy quark masses and of α_s on the uncertainties of the Higgs branching fractions in various channels. One finds partially large effects as 6 % from M_c on the $H \to c\bar{c}$ branching or 5.6 % from α_s on $H \to gg$. These will certainly be much reduced. It is for future studies to more systematically analyse the striking potential of the LHeC to remove or reduce the QCD uncertainties of the Higgs cross sections and couplings. There will also be improvements related to QCD measurements at the LHC. Their level of precision, however, especially for the gluon, α_s and heavy quark QCD cannot compete with the genuine DIS process.

It has also been observed [1], that the LHeC can specifically explore well the CP structure of the HWW coupling by separating it from the HZZ coupling and the other signal production mechanisms. Any determination of an anomalous HWW vertex will thus be free from possible contaminations of these. A further advantage of the ep collider kinematics stems from the ability to disentangle clearly the direction of the struck parton and the final state lepton (clear definition of forward and backward directions). Compared to the pp situation, ep lacks the complications due to underlying event and pile-up driven backgrounds.

The few initial studies performed so far will be pursued further given that the Higgs boson is now likely to indeed exist. For the projected analyses, this first concerns using the appropriate LHeC detector simulation, and optimising further its design. For the accelerator design it is obvious that a luminosity in excess of 10^{33} cm^{-2}s^{-1} is very desirable, see the discussion on machine parameters in Section 2. The then possible precision measurements of rarer (τ, Z, W, perhaps photon) decay channels, of the CP angular distributions, for both the HWW and HZZ couplings, and NC initiated production would make the LHeC, by design a QCD machine, a collider to study the Higgs boson and mechanism of very remarkable and complementary potential. The assistance in removing a large part of the QCD and PDF related uncertainties of the Higgs measurements in pp will help making the LHC a genuine precision Higgs facility.

6 Heavy Ion Physics

As discussed in [1], the study of eA collisions at the LHeC will have strong implications on physics of ultrarelativistic heavy-ion collisions presently studied at RHIC and at the LHC. This applies both to the

initial state which determines the subsequent behaviour of the dense medium produced in the collisions, and to the ability of hard probes to characterize such medium. Different physical effects need to be cleanly separated, that are not due to the presence of a medium, like nuclear modifications of parton densities or details of the mechanism of particle production. Finally, it is also crucial to understand how the medium affects the probe, for example the mechanism of QCD radiation and parton energy loss in a medium.

6.1   Aspects of heavy-ion physics that can be addressed in eA at the LHeC

Currently, nuclear parton distribution functions (nPDFs) suffer from large uncertainties due to the very limited coverage in the kinematics obtained by the measurements in low-energy fixed-target experiments. As a result, gluon and quark distribution functions are presently almost unconstrained for values of x below 10^{-2}, which translates into uncertainties in the precise characterization of the medium in heavy-ion collisions through hard probes e.g. J/Ψ production [22].

The LHeC will provide an unprecedented precision for the measurement of the parton content of nuclei. The kinematic coverage for eA collisions at the LHeC will allow to extend the x and Q^2 ranges by 3 to 4 orders of magnitude down to $x \sim 10^{-5} - 10^{-6}$ and up to $Q^2 \sim 10^6$ GeV^2 respectively, see [1,2]. Flavor decomposition of the nuclear structure functions will be performed for the first time, including the measurement of the previously unknown charm and beauty components of nPDFs. An example of the constraining power of the LHeC is illustrated in Fig. 6 (left) where the nuclear modification factor is shown for the gluon distribution as a function of x for a fixed value of Q^2. Clearly, the LHeC offers huge possibilities for distinguishing between different models of nuclear shadowing and for constraining the nuclear parton dynamics, particularly at small values of x. Note also that diffraction in ep and nuclear shadowing are theoretically related through Gribov relation that can be cleanly tested at the LHeC. Finally, access to large values of $x > 0.1$ will also be possible at the LHeC, thus providing additional information about the antishadowing and EMC effects for nuclear ratios.

Ultrarelativistic heavy-ion collisions at RHIC and the LHC allow to create and characterize partonic matter under extreme conditions. The description of the collective behaviour of such matter involves several stages, which include modeling the initial conditions prior to isotropization, the subsequent evolution of the system through relativistic hydrodynamics and, finally, hadronisation. The initial conditions for the heavy ion collisions are currently being parametrized and fitted to the data. They involve large uncertainties which translate into the uncertainties of the extracted bulk properties of the medium such as shear viscosity [23]. The LHeC offers unique possibilities for pinning down these initial conditions. The initial state can be determined through the details of nPDFs and of particle production, both measured precisely in eA collisions. Furthermore, there are sound theoretical indications that at low x and for large nuclei, a novel regime of QCD appears that is characterized by high parton densities. In this regime, the standard collinear framework that was developed for a dilute parton system must break down and should be superseded by a more complicated, non-linear evolution setup that leads to the saturation of parton densities. The existence and properties of this partonic dense regime will be tested at the LHeC through several measurements ranging from those of structure functions, with subsequent determination of parton distribution functions in nuclei (see Fig. 6 (left)) and inclusive diffraction to more exclusive ones such as elastic vector meson production (Fig. 6 (center)). Thus it will be possible to locate the onset of the saturation regime as a function of x, mass number and impact parameter of the collision. Remarkably, and unlike in lower energy facilities, at the LHeC this phenomenon can be investigated in the DIS region where the coupling is small and perturbative techniques are applicable to the non-linear regime. Furthermore, saturation can be observed both in ep and eA, which gives a unique possibility for disentangling saturation from other nuclear effects.

Finally, one of the standard tools for characterizing the medium created in heavy-ion collisions is the modification of the yield of high-energy particles - jet quenching - due to the changes in QCD radiation and hadronization induced by the presence of a dense medium. Such characterization demands a detailed understanding of these phenomena that can be achieved by studying particle and jet yields and correlations in eA collisions at the LHeC. In this respect, the kinematics of the parton whose radiation and hadronization undergoes medium modifications is much more precisely constrained in DIS than in hadronic collisions. As an example, the large kinematic range of LHeC allows to investigate the dynamics of partons traveling through
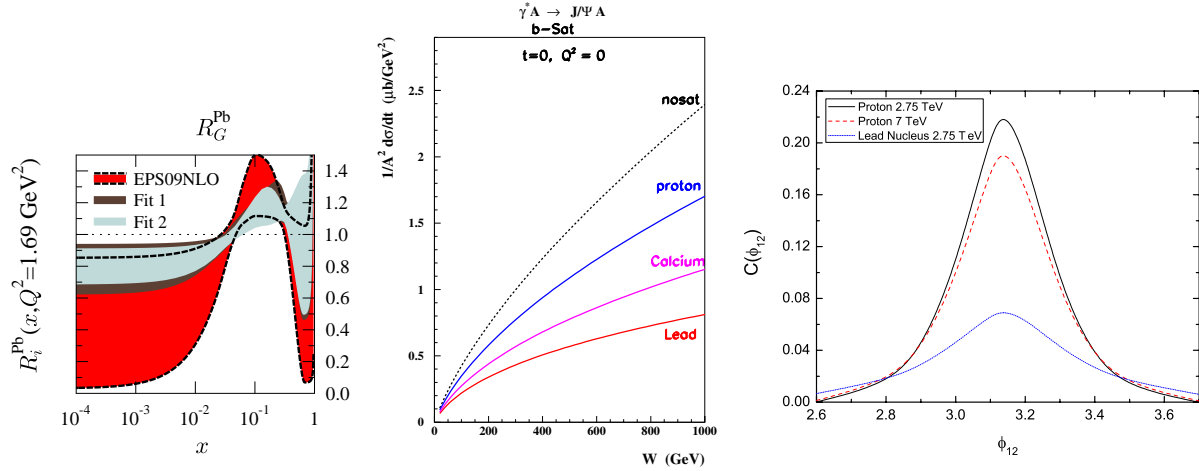
Figure 6: Left: Ratio of gluon density for protons bound in Pb to those in a free proton at $Q^2 = 1.69$ GeV^2. The red band corresponds to the uncertainty in the original EPS09 analysis, while the brown band corresponds to the uncertainty obtained after including nuclear LHeC pseudodata on the total reduced cross sections (Fit 1). The light blue band corresponds to the uncertainty after including the information on charm and beauty cross sections (Fit 2). Center: Energy (W) dependence of the coherent photoproduction of the J/Ψ on a proton and different nuclei in the forward case $t = 0$ according to the b-Sat model. Right: Di-hadron correlation function for the case of the scattering off the proton (red-dashed and black-solid lines) compared to the eA case (blue-dotted line). The energy of the electron is assumed to be $E_e = 50$ GeV. The observed hadrons are pions. See [1] for details.

the nucleus with energies from moderate to very large. Besides, the study of particle angular correlations (e.g. back-to-back ones, Fig. 6 (right)) will offer insight both on these changes and on the possible breakdown of collinear factorization and the existence of a dense partonic regime.

6.2 Prospects in pPb collisions at the LHC compared to ePb at the LHeC

A first pPb run at the LHC is scheduled for early 2013 (a pilot run providing $\mathcal{O}(10^6)$ collisions per experiment happened last September 13th 2012 and one publication already appeared [24]). Tentative plans exists for additional runs in the future [25]. They offer information [26] about similar aspects relevant for heavy-ion collisions to those discussed here for eA at the LHeC. The $x - Q^2$ region explored at the LHC with forward instrumentation both in hadronic and ultraperipheral collisions, and at the LHeC, will be comparable [1, 26]

Nevertheless, even assuming that corrections to collinear factorization are small - though they are expected to be larger in pA than in pp, the nuclear modifications of partonic densities and of fragmentation and hadronization, come intrinsically mixed for most observables in pA collisions, see e.g. the discussion in [27]. Therefore, they will be far more difficult to constrain in pPb at the LHC than in ePb at the LHeC. Besides, the accuracy - of a few percent - for measurements of cross sections achievable at the LHeC cannot be matched in a pA collider. Finally, the determination of the kinematic variables relevant for parton densities, fragmentation functions and other quantities of interest, is much more direct in DIS than in hadronic collisions. Thus, the information that can be obtained in ePb collisions at the LHeC will be substantially more precise, and the possibilities for discovery of the dense regime of QCD at small x through quantitative studies as those proposed in [1] significantly larger, than in pPb collisions at the LHC.

16

7 Summary

The LHeC is a new ep collider of unprecedent kinematic range, luminosity and precision in deep inelastic scattering. This leads to the first ever complete measurement of PDFs, including, for example, the strange density. It furthermore extends to very high Bjorken x in ep and to so large Q^2 that no nuclear or higher twist corrections affect the high x PDF determinations. A much deeper understanding of quark-gluon dynamics is needed and in sight, exemplified by the potential of the LHeC to measure $\alpha_s(M_Z^2)$ to per mille accuracy.

The LHeC is designed to operate synchronously with the HL-LHC. Preparations have begun, following the detailed design concept report and a corresponding mandate from CERN, supported by ECFA and NuPECC, to prototype critical components and to carry out more detailed studies, as of the interaction region and high luminosity optics, in major international collaborations with CERN. As has been indicated here, there is a potential for the LHeC to achieve luminosities in excess of $10^{33}\,\mathrm{cm}^{-2}\mathrm{s}^{-1}$. The formation of a detector collaboration has indeed begun.

The present paper discussed the relation of the LHeC to the LHC, in its HL phase. As indicated by the ATLAS contribution to the ESPP, there are two major questions for the HL-LHC to investigate, the properties of the 126 GeV boson, which likely is the Higgs particle, and the search for maximum mass particles, of several TeV in direct production mode. It has been argued here that the LHeC can assist the transformation of the LHC into a precision Higgs facility, with its own coupling and CP measurements based on clean WW fusion in ep, and with its ultra-precise PDF, heavy quark and α_s determinations, which will reduce the theoretical uncertainties of Higgs measurements in pp to a negligible level. It is similarly apparent that the discovery potential of new particles at high masses at the HL-LHC is severely limited by the deviations and uncertainties of the predictions based on currently available PDF sets and as well the uncertainties of input parameters such as the heavy quark masses and α_s. For the Higgs the prominent decay $H \to b\bar{b}$ and for SUSY gluino pair production have been used as first representative examples.

It has been also discussed which role DIS and Drell-Yan scattering can play in the determination of PDFs, which may be illustrated by comparing the HERA and Tevatron PDF related results. Obviously ep provides precision information on the quark structure and quark-gluon dynamics while the prime task of pp is the extension of the energy frontier. With the Higgs measurements and BSM searches at the LHC, these aspects appear intimately connected, stronger than before, because both pp and ep, owing to higher energies and huge luminosities, can explore the high mass limits of phase space.

The paper has also summarised the importance of electron-ion scattering for the LHC heavy ion physics programme, with the determination of nuclear PDFs in a phase space extended by 4 orders of magnitude and diversified with heavy quark nPDFs to be measured for the first time. The LHeC determines the initial state of the QGM and leads to a quantitative understanding of the hadronisation in media, controlled by the electron DIS kinematics.

The LHeC has its own, fundamental physics programme, as with saturation and diffractive physics, with the resolution of deuteron, neutron and photon structure, for example. Its relation to the LHC extends beyond the nowadays most prominent examples, Higgs measurements and SUSY searches, as with top, leptoquark, excited lepton or electroweak physics. The CDR has demonstrated that the LHeC may be realised without any major extra machine delays. Pairing the unique hadron beams of the LHC with a new lepton beam would therefore substantially enrich the physics potential of the LHC facility and make optimum use of the major investment already made and envisaged for the LHC.

References

[1] J. L. Abelleira Fernandez *et al.* [LHeC Study Group], "A Large Hadron Electron Collider at CERN" J.Phys.G. **39**(2012)075001, arXiv:1206.2913.

[2] LHeC Study Group, Contribution (No 147) to the Cracow meeting on the ESPP, "A Large Hadron Electron Collider at CERN", LHeC-Note-2012-004 GEN, CERN, August 2012.

[3] G. Aad *et al.* [ATLAS Collaboration], Phys. Lett. B **716** (2012) 1 [arXiv:1207.7214 [hep-ex]].

[4] S. Chatrchyan *et al.* [CMS Collaboration], Phys. Lett. B **716** (2012) 30 [arXiv:1207.7235 [hep-ex]].

[5] ATLAS Collaboration, Contributions to the ESPP, "Physics at High Luminosity LHC with ATLAS", CERN, August 2012 and Update October 2012.

[6] J. Collins, "Foundations of perturbative QCD, (Cambridge U.P., Cambridge, 2011)

[7] H. -L. Lai, M. Guzzi, J. Huston, Z. Li, P. M. Nadolsky, J. Pumplin and C. -P. Yuan, Phys. Rev. D **82** (2010) 074024 [arXiv:1007.2241 [hep-ph]].

[8] A. D. Martin, W. J. Stirling, R. S. Thorne and G. Watt, Eur. Phys. J. C **63** (2009) 189 [arXiv:0901.0002 [hep-ph]].

[9] R. D. Ball *et al.* [NNPDF Collaboration], Nucl. Phys. B **855** (2012) 153 [arXiv:1107.2652 [hep-ph]].

[10] S. Forte, Acta Phys. Polon. B **41** (2010) 2859 [arXiv:1011.5247 [hep-ph]].

[11] S. Alekhin, J. Blümlein and S. Moch, Phys. Rev. D **86** (2012) 054009 [arXiv:1202.2281 [hep-ph]].

[12] M. Wobisch, private communication, see also
D. Bandurin, Plenary Talk on QCD at ICHEP2012, Melbourne (2012).

[13] S. S. AbdusSalam, B. C. Allanach, H. K. Dreiner, J. Ellis, U. Ellwanger, J. Gunion, S. Heinemeyer and M. Kraemer *et al.*, Eur. Phys. J. C **71** (2011) 1835 [arXiv:1109.3859 [hep-ph]].

[14] B. C. Allanach, Comput. Phys. Commun. **143** (2002) 305 [hep-ph/0104145].

[15] W. Beenakker, R. Hopker, M. Spira and P. M. Zerwas, Nucl. Phys. B **492** (1997) 51 [hep-ph/9610490].

[16] Prospino, $http://www.thphys.uni-heidelberg.de/plehn/...$ see tools;
R. Kleiss, Master thesis, University of Heidelberg (unpublished).

[17] H. K. Dreiner, M. Kraemer, J. M. Lindert and B. O'Leary, JHEP **1004** (2010) 109 [arXiv:1003.2648 [hep-ph]].

[18] J. Baglio, A. Djouadi and R. M. Godbole, Phys. Lett. B **716** (2012) 203 [arXiv:1207.1451 [hep-ph]].

[19] J. Rojo, Talk at the PDF4LHC Workshop, 8th of October, 2012, CERN.

[20] J. Baglio and A. Djouadi, JHEP **1103** (2011) 055 [arXiv:1012.0530 [hep-ph]].

[21] A. Denner, S. Heinemeyer, I. Puljak, D. Rebuzzi and M. Spira, Eur. Phys. J. C **71** (2011) 1753 [arXiv:1107.5909 [hep-ph]].

[22] B. Abelev *et al.* [ALICE Collaboration], Phys. Rev. Lett. **109** (2012) 072301 [arXiv:1202.1383 [hep-ex]].

[23] C. Shen, S. A. Bass, T. Hirano, P. Huovinen, Z. Qiu, H. Song and U. Heinz, J. Phys. G **38** (2011) 124045 [arXiv:1106.6350 [nucl-th]].

[24] B. Abelev *et al.* [ALICE Collaboration], arXiv:1210.3615 [nucl-ex].

[25] J. M. Jowett, "LHC heavy ion programme", contribution no. 164 to the Open Symposium of the European Strategy Preparatory Group (10-12 September 2012, Krakow, Poland).

[26] C. A. Salgado, J. Alvarez-Muniz, F. Arleo, N. Armesto, M. Botje, M. Cacciari, J. Campbell and C. Carli *et al.*, J. Phys. G **39** (2012) 015010 [arXiv:1105.3919 [hep-ph]].

[27] K. J. Eskola, arXiv:1209.1546 [hep-ph].

LHeC Study Group

J.L.Abelleira Fernandez[16,23], C.Adolphsen[57], P.Adzic[74], A.N.Akay[03], H.Aksakal[39], J.L.Albacete[52], B.Allanach[73], S.Alekhin[17,54], P.Allport[24], V.Andreev[34], R.B.Appleby[14,30], E.Arikan[39], N.Armesto[53,a], G.Azuelos[33,64], M.Bai[37], D.Barber[14,17,24], J.Bartels[18], O.Behnke[17], J.Behr[17], A.S.Belyaev[15,56], I.Ben-Zvi[37], N.Bernard[25], S.Bertolucci[16], S.Bettoni[16], S.Biswal[41], J.Blümlein[17], H.Böttcher[17], A.Bogacz[36], C.Bracco[16], J.Bracinik[06], G.Brandt[44], H.Braun[65], S.Brodsky[57,b], O.Brüning[16], E.Bulyak[12], A.Buniatyan[17], H.Burkhardt[16], I.T.Cakir[02], O.Cakir[01], R.Calaga[16], A.Caldwell[70], V.Cetinkaya[01], V.Chekelian[70], E.Ciapala[16], R.Ciftci[01], A.K.Ciftci[01], B.A.Cole[38], J.C.Collins[48], O.Dadoun[42], J.Dainton[24], A.De.Roeck[16], D.d'Enterria[16], P.DiNezza[72], A.Dudarev[16], A.Eide[60], R.Enberg[63], E.Eroglu[62], K.J.Eskola[21], L.Favart[08], M.Fitterer[16], S.Forte[32], A.Gaddi[16], P.Gambino[59], H.García Morales[16], T.Gehrmann[69], P.Gladkikh[12], C.Glasman[28], A.Glazov[17], R.Godbole[35], B.Goddard[16], T.Greenshaw[24], A.Guffanti[13], V.Guzey[19,36], C.Gwenlan[44], T.Han[50], Y.Hao[37], F.Haug[16], W.Herr[16], A.Hervé[27], B.J.Holzer[16], M.Ishitsuka[58], M.Jacquet[42], B.Jeanneret[16], E.Jensen[16], J.M.Jimenez[16], J.M.Jowett[16], H.Jung[17], H.Karadeniz[02], D.Kayran[37], A.Kilic[62], K.Kimura[58], R.Klees[75], M.Klein[24], U.Klein[24], T.Kluge[24], F.Kocak[62], M.Korostelev[24], A.Kosmicki[16], P.Kostka[17], H.Kowalski[17], M.Kraemer[75], G.Kramer[18], D.Kuchler[16], M.Kuze[58], T.Lappi[21,c], P.Laycock[24], E.Levichev[40], S.Levonian[17], V.N.Litvinenko[37], A.Lombardi[16], J.Maeda[58], C.Marquet[16], B.Mellado[27], K.H.Mess[16], A.Milanese[16], J.G.Milhano[76], S.Moch[17], I.I.Morozov[40], Y.Muttoni[16], S.Myers[16], S.Nandi[55], Z.Nergiz[39], P.R.Newman[06], T.Omori[61], J.Osborne[16], E.Paoloni[49], Y.Papaphilippou[16], C.Pascaud[42], H.Paukkunen[53], E.Perez[16], T.Pieloni[23], E.Pilicer[62], B.Pire[45], R.Placakyte[17], A.Polini[07], V.Ptitsyn[37], Y.Pupkov[40], V.Radescu[17], S.Raychaudhuri[35], L.Rinolfi[16], E.Rizvi[71], R.Rohini[35], J.Rojo[16,31], S.Russenschuck[16], M.Sahin[03], C.A.Salgado[53,a], K.Sampei[58], R.Sassot[09], E.Sauvan[04], M.Schaefer[75], U.Schneekloth[17], T.Schörner-Sadenius[17], D.Schulte[16], A.Senol[22], A.Seryi[44], P.Sievers[16], A.N.Skrinsky[40], W.Smith[27], D.South[17], H.Spiesberger[29], A.M.Stasto[48,d], M.Strikman[48], M.Sullivan[57], S.Sultansoy[03,e], Y.P.Sun[57], B.Surrow[11], L.Szymanowski[66,f], P.Taels[05], I.Tapan[62], T.Tasci[22], E.Tassi[10], H.Ten.Kate[16], J.Terron[28], H.Thiesen[16], L.Thompson[14,30], P.Thompson[06], K.Tokushuku[61], R.Tomás García[16], D.Tommasini[16], D.Trbojevic[37], N.Tsoupas[37], J.Tuckmantel[16], S.Turkoz[01], T.N.Trinh[47], K.Tywoniuk[26], G.Unel[20], T.Ullrich[37], J.Urakawa[61], P.VanMechelen[05], A.Variola[52], R.Veness[16], A.Vivoli[16], P.Vobly[40], J.Wagner[66], R.Wallny[68], S.Wallon[43,46,f], G.Watt[69], C.Weiss[36], U.A.Wiedemann[16], U.Wienands[57], F.Willeke[37], B.-W.Xiao[48], V.Yakimenko[37], A.F.Zarnecki[67], Z.Zhang[42], F.Zimmermann[16], R.Zlebcik[51], F.Zomer[42]

01 *Ankara University, Turkey*
02 *SANAEM Ankara, Turkey*
03 *TOBB University of Economics and Technology, Ankara, Turkey*
04 *LAPP, Annecy, France*
05 *University of Antwerp, Belgium*
06 *University of Birmingham, UK*
07 *INFN Bologna, Italy*
08 *IIHE, Université Libre de Bruxelles, Belgium, supported by the FNRS*
09 *University of Buenos Aires, Argentina*
10 *INFN Gruppo Collegato di Cosenza and Universita della Calabria, Italy*
11 *Massachusetts Institute of Technology, Cambridge, USA*
12 *Charkow National University, Ukraine*
13 *University of Copenhagen, Denmark*
14 *Cockcroft Institute, Daresbury, UK*
15 *Rutherford Appleton Laboratory, Didcot, UK*
16 *CERN, Geneva, Switzerland*
17 *DESY, Hamburg and Zeuthen, Germany*
18 *University of Hamburg, Germany*
19 *Hampton University, USA*
20 *University of California, Irvine, USA*
21 *University of Jyväskylä, Finland*
22 *Kastamonu University, Turkey*
23 *EPFL, Lausanne, Switzerland*
24 *University of Liverpool, UK*
25 *University of California, Los Angeles, USA*
26 *Lund University, Sweden*
27 *University of Wisconsin-Madison, USA*
28 *Universidad Autónoma de Madrid, Spain*
29 *University of Mainz, Germany*
30 *The University of Manchester, UK*
31 *INFN Milano, Italy*
32 *University of Milano, Italy*
33 *University of Montréal, Canada*
34 *LPI Moscow, Russia*
35 *Tata Institute, Mumbai, India*
36 *Jefferson Lab, Newport News, VA 23606, USA*
37 *Brookhaven National Laboratory, New York, USA*
38 *Columbia University, New York, USA*
39 *Nigde University, Turkey*

[40] *Budker Institute of Nuclear Physics SB RAS, Novosibirsk, 630090 Russia*
[41] *Orissa University, India*
[42] *LAL, Orsay, France*
[43] *Laboratoire de Physique Théorique, Université Paris XI, Orsay, France*
[44] *University of Oxford, UK*
[45] *CPHT, École Polytechnique, CNRS, 91128 Palaiseau, France*
[46] *UPMC University of Paris 06, Faculté de Physique, Paris, France*
[47] *LPNHE University of Paris 06 and 07, CNRS/IN2P3, 75252 Paris, France*
[48] *Pennsylvania State University, USA*
[49] *University of Pisa, Italy*
[50] *University of Pittsburgh, USA*
[51] *Charles University, Praha, Czech Republic*
[52] *IPhT Saclay, France*
[53] *University of Santiago de Compostela, Spain*
[54] *Serpukhov Institute, Russia*
[55] *University of Siegen, Germany*
[56] *University of Southampton, UK*
[57] *SLAC National Accelerator Laboratory, Stanford, USA*
[58] *Tokyo Institute of Technology, Japan*
[59] *University of Torino and INFN Torino, Italy*
[60] *NTNU, Trondheim, Norway*
[61] *KEK, Tsukuba, Japan*
[62] *Uludag University, Turkey*
[63] *Uppsala University, Sweden*
[64] *TRIUMF, Vancouver, Canada*
[65] *Paul Scherrer Institute, Villigen, Switzerland*
[66] *National Center for Nuclear Research (NCBJ), Warsaw, Poland*
[67] *University of Warsaw, Poland*
[68] *ETH Zurich, Switzerland*
[69] *University of Zurich, Switzerland*
[70] *Max Planck Institute Werner Heisenberg, Munich, Germany*
[71] *QMW University London, United Kingdom*
[72] *Laboratori Nazionali di Frascati, INFN, Italy*
[73] *DAMTP, CMS, University of Cambridge, United Kingdom*
[74] *University of Belgrade, Serbia*
[75] *RWTH Aachen University, Germany*
[76] *Instituto Superior Técnico, Universidade Técnica de Lisboa, Portugal*

20